

Investigation of a Natural Gas / Low-Enthalpy Geothermal Energy Hybrid System

Thomai-Komnini Dermata, Lydia Schina, Apostolos Gkountas, Nikolaos Andritsos

Department of Mechanical Engineering, University of Thessaly, Leoforos Athinon, GR 38334, Volos, Greece

nandrits@uth.gr

Keywords: energy production, direct uses, exergy analysis, economic analysis.

ABSTRACT

In Northern Greece there are several low-enthalpy geothermal fields with water temperatures reaching 100°C. These waters only marginally can be exploited as heat sources for power generation, using a binary cycle conversion system. This paper examines the production of 4 MWe from low temperature geothermal resources in combination with natural gas in the geothermal field of Aristino (Thrace). Three systems have been considered. The first system combines low-enthalpy geothermal energy and natural gas superheating. The second systems is a natural gas plant and the third one combines geothermal energy and natural gas Brayton cycle. The assessment of these systems was based on energy, exergy and economic analysis. The results of the analysis show that it is quite economical to “upgrade” low-to-medium temperature geothermal waters for electricity production using a binary cycle.

1. INTRODUCTION

Greece, like many other Mediterranean countries (e.g. Italy and Turkey) is rich in geothermal energy. This is because the greatest part of the country is located in an area geodynamically very active, as a result of the movement of the African plate towards the Eurasian plate.

The high enthalpy geothermal resources appear to be confined in the active South Aegean volcanic arc, with a proven potential exceeding 250 MWe in the islands of Milos and Nisyros. However, no geothermal power is produced in the country and it can be attributed partially to the negative sentiment of the people of these islands towards geothermal development after the shut-down in 1989 of the ill-fated 2 MWe power plant in Milos Island.

Low-enthalpy geothermal fields (with water temperature less than 100 °C) are numerous in Greece, most of which are located in some basins in Northern Greece, as well as in many Aegean islands. Present data indicate that the proven low enthalpy potential in the country exceeds 1000 MWt. However, only a

small share of this potential is currently exploited (Andritsos et al., 2015)

Most of the low-enthalpy fields are located at very shallow depths (100-500 m) in the post-orogenic basins (e.g. basins of Nestos River, Strymon River and Evros River) and in the islands of Samothrace, Chios and Lesbos (Fytikas and Kolios, 1992; Kolios et al., 2007; Mendrinos et al., 2010). The most important of these fields are shown in Fig. 1. The geological and tectonic conditions in these areas are favourable for the presence of medium-enthalpy geothermal fields ($T=90-120$ °C) at greater depths. Obviously, further exploration is needed with deeper wells, something that is rather improbable considering the economic situation of the country.



Figure 1: Location of the most promising geothermal fields.

Over the past two decades there is plethora of papers dealing with the theoretical investigation of using geothermal energy for power generation in combination with other energy sources in order to achieve higher power production with lower exploration risk. For example, geothermal energy can be combined with coal-fired power plants (e.g. DiPippo, 2015), with solar energy, with biomass and with natural gas. On the other hand, only a limited number of such hybrid systems are currently in use.

One of the best examples is the hybrid biomass-geothermal system in Castelnuovo Val di Cecina, Tuscany, Italy (Romagnoli, 2016.) A 5-MW biomass plant helps to increase the temperature of the steam generated from the geothermal site from 150°-160°C to 370°-380°C.

The scope of the paper is to analyse and assess the possibility of using the existing geothermal waters in the range 90-100 °C for electricity generation in conjunction with natural gas. In recent years several scenarios have been described for using geothermal energy (mostly medium-enthalpy) in hybrid systems. To explore this possibility, the geothermal field of Aristino in Thrace was considered, which lies next to main natural gas transmission pipeline entering from the Greek-Turkish border.

The Aristino field is located east of Alexandroupoli and west of the tertiary basin of the river Evros and it is characterized by particularly intense tectonic activity coupled with major development of tertiary volcanism. The geothermal resources of the field are in liquid state and have a temperature of 30 to 95°C. The confirmed geothermal field covers an area of 20 km² and the depth of the reservoir is 150-450 m. The geothermal waters in the Aristino field are of the Na-Cl type in chemical composition. Their TDS values range from 4.3 to 10.5 g/l and their Ca²⁺ and SO₄²⁻ contents are relatively high (Kolios et al., 2005).

2. GEOTHERMAL HYBRID SYSTEMS

Three systems are considered in our analysis.

2.1 System 1: Hybrid system of low-enthalpy geothermal energy and natural gas superheating

This hybrid system comprises of three subsystems, as it is shown in Figure 2. Heat is transferred from both

the subsystem of the geothermal resource and the subsystem of the natural gas to the working organic fluid of an ORC through heat exchangers.

(1) Subsystem of geothermal fluid (1-2-4): The geothermal fluid transfers its heat through the evaporator to the working organic fluid and returns to the natural reservoir.

(2) Organic Rankine Cycle (3-5-6-7-8): The selected organic fluid is isobutane due to its properties (e.g. boiling point) that make it an ideal working fluid for this system. The working fluid receiving heat from the geothermal resource evaporates and then flows through a second heat exchanger where it is superheated by the combustion gases of the natural gas. Finally, it is expanded in a turbine, producing electricity, and cooled in a water-cooled condenser.

(3) Subsystem of the natural gas (11-12-13).

The most important parameters of this hybrid system are as follows:

- geothermal mass flow: $\dot{m}_{geo} = 55.56 \text{ kg/s}$
- organic fluid mass flow: $\dot{m}_{orc} = 30 \text{ kg/s}$
- natural gas mass flow: $\dot{m}_b = 0.7448 \text{ kg/s}$
- target electricity production : $P_T = 4 \text{ MW}$
- geothermal fluid enters the system at 90°C (363 K) and 2.5 bar
- temperature of the exhaust gas: 753.6 K
- maximum temperature of the Rankine cycle (before the expansion in the turbine): 455 K.

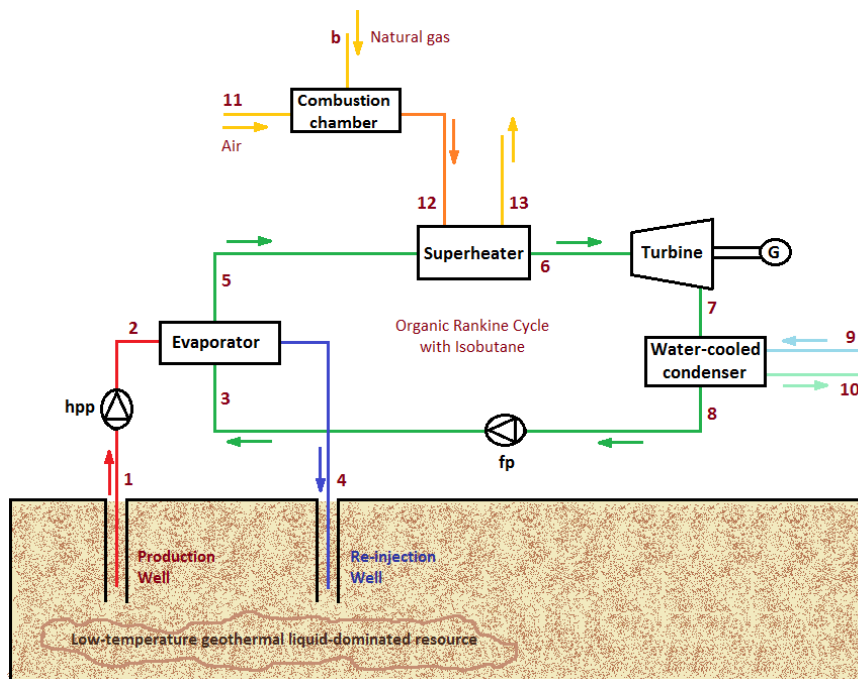


Figure 2: System 1 – Hybrid Geothermal System with natural gas superheating.

2.2 System 2: Natural gas plant

The second system under consideration is a natural gas plant (Figure 3) that consists of a typical open Brayton cycle, which includes a compressor, a combustion chamber and a turbine.

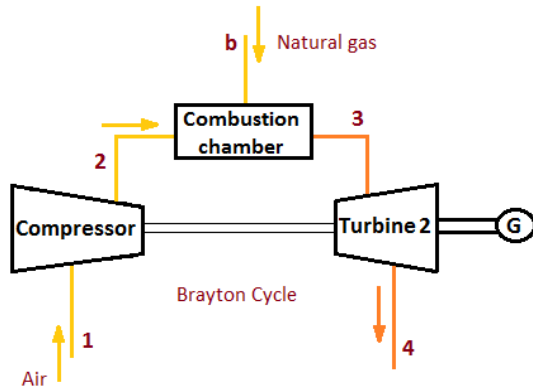


Figure 3: System 2 – Natural Gas Brayton cycle.

Again, the main parameters of this system are as follows:

- target electricity production $P_{net} = 4$ MW
- natural gas mass flow $\dot{m}_b = 1.885$ kg/s
- maximum temperature of the Brayton cycle is 963.9 K, whereas the minimum temperature is 293 K
- pressure ratio in the compressor and turbine = 5
- lower heating value of the natural gas: 46000 kJ/kg

2.3 System 3: Hybrid system of low-enthalpy geothermal energy and natural gas superheating

This hybrid system again comprises of three subsystems, as shown in Fig. 3.

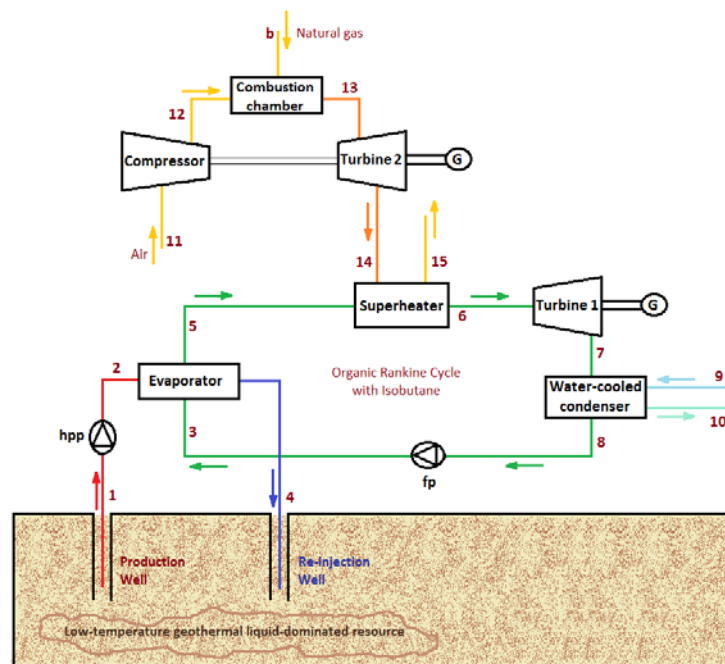


Figure 4: System 3 –Hybrid Geothermal System with natural gas power production.

(1) The subsystem of the geothermal fluid (1-2-4): The geothermal fluid transfers its heat through the evaporator to the working organic fluid.

(2) The Organic Rankine Cycle (3-5-6-7-8): The isobutane was selected as the organic fluid. The working fluid evaporates and then flows through a second heat exchanger, where it is superheated using natural gas as heating fluid. Finally, it is expanded in a turbine, producing electricity, and fully condensed in a water-cooled heat exchanger.

(3) The subsystem of Brayton cycle (11-12-13-14-15): It includes a compressor, a combustion chamber and a turbine. The atmospheric air once compressed enters the combustion chamber along with the natural gas and the product of combustion is expanded in a turbine for the extra production of electricity. Finally, the exhaust gas superheats the working fluid of the ORC cycle through the second heat exchanger.

The most important parameters of this hybrid system are as follows:

- geothermal mass flow: $\dot{m}_{geo} = 55.56$ kg/s
- organic fluid mass flow: $\dot{m}_{orc} = 20$ kg/s
- natural gas mass flow: $\dot{m}_b = 0.6435$ kg/s
- target of electricity production: $(\dot{W}_t + P_{net}) = 4$ MW
- geothermal fluid enters the system at 90°C (363 K) and 2.5 bar
- maximum temperature of the Brayton cycle is 963.9 K
- pressure ratio in the air compressor and the turbine: 5
- maximum temperature of the Rankine cycle (before the expansion in the turbine) is 455 K.

3. ENERGY ANALYSIS

3.1 Rankine cycle

The turbine power of the Rankine cycle is

$$\dot{W}_t = \dot{m}_{orc} \cdot (h_{in} - h_{out}) \quad (\text{kW}) \quad [1]$$

The power consumed by the feed pump and by the high pressure pump in the subsystem of the geothermal fluid is calculated as follows:

$$\dot{W}_{fp,hpp} = \frac{\dot{m} \cdot (P_{dis} - P_{suction})}{\rho \cdot \eta_{pump} \cdot 100} \quad (\text{kW}) \quad [2]$$

where $\eta_{pump} = 0.85$, ρ (kg/m³) is the mean density of the fluid and P (bar) the suction and discharge pressure of the pump.

The heat balance equations of the heat exchangers are expressed below as a function of the mass flow and the difference between enthalpies of the two fluid currents:

Evaporator:

$$\dot{m}_{geo} \cdot (h_{geo,in} - h_{geo,out}) = \dot{m}_{orc} \cdot (h_{orc,out} - h_{orc,in}) \quad [3]$$

Condenser:

$$\dot{m}_{orc} \cdot (h_{orc,in} - h_{orc,out}) = \dot{m}_{water} \cdot (h_{water,out} - h_{water,in}) \quad [4]$$

Superheater:

$$\dot{m}_A \cdot (h_{A,in} - h_{A,out}) = \dot{m}_{orc} \cdot (h_{orc,out} - h_{orc,in}) \quad [5]$$

where \dot{m}_A is the exhaust gas mass flow of natural gas combustion and \dot{m}_{water} the water mass flow in the water-cooled condenser.

The thermal efficiency of the ORC and of the plant is determined by the following formula:

$$\eta_{th,orc} = \left(\frac{\dot{W}_t - \dot{W}_{pumps}}{\dot{m}_{geo} \cdot (h_{geo,in} - h_{geo,out}) + \dot{m}_A \cdot (h_{A,in} - h_{A,out})} \right) \quad [6]$$

3.2 Brayton cycle

The thermal efficiency of the Brayton cycle is calculated as follows:

$$\eta_{th} = \frac{w_{net}}{q} \quad [7]$$

where q is the specific heat (kJ/kg) that is produced by the combustion chamber, $q = h_{out} - h_{in}$, w_{net} the specific net work of the cycle (kJ/kg), $w_{net} = w_{tg} - w_c$, $w_{tg} = n_m \cdot (h_{tg,in} - h_{tg,out})$ the specific work of the turbine, $w_c = (h_{c,out} - h_{c,in})$ the specific work of the compressor and n_m the mechanical efficiency.

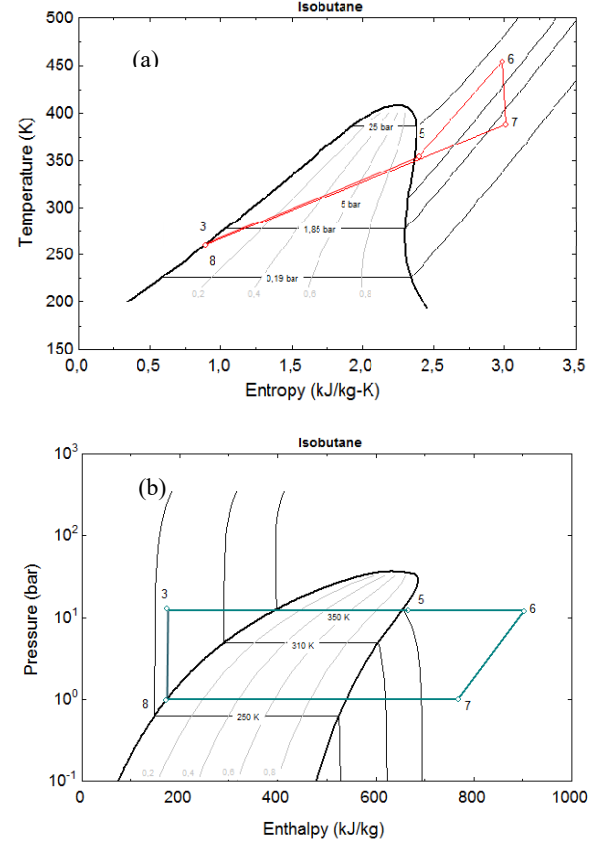


Figure 5: T-s (a) and P-h (b) diagrams of isobutane in the systems 1 and 3.

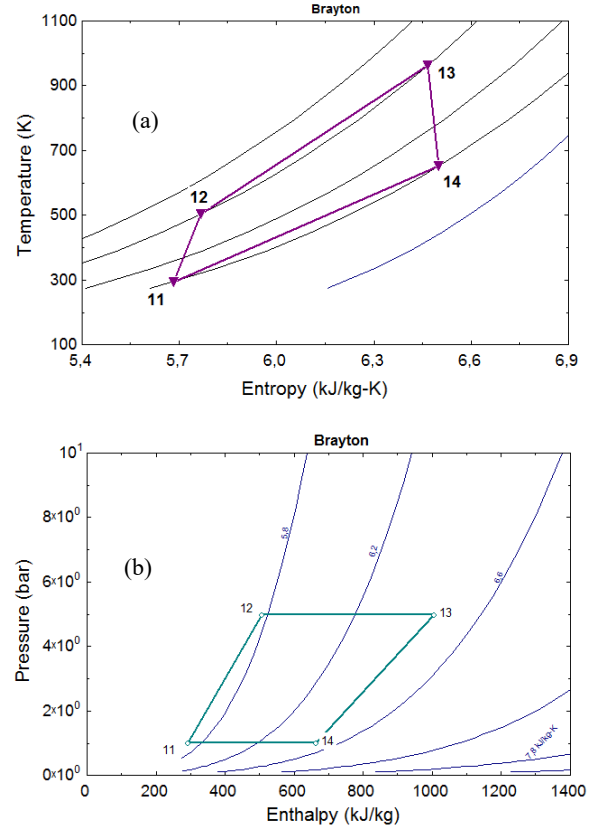


Figure 6: T-s (a) and P-h (b) diagrams of the Brayton cycle of the systems 1 and 3.

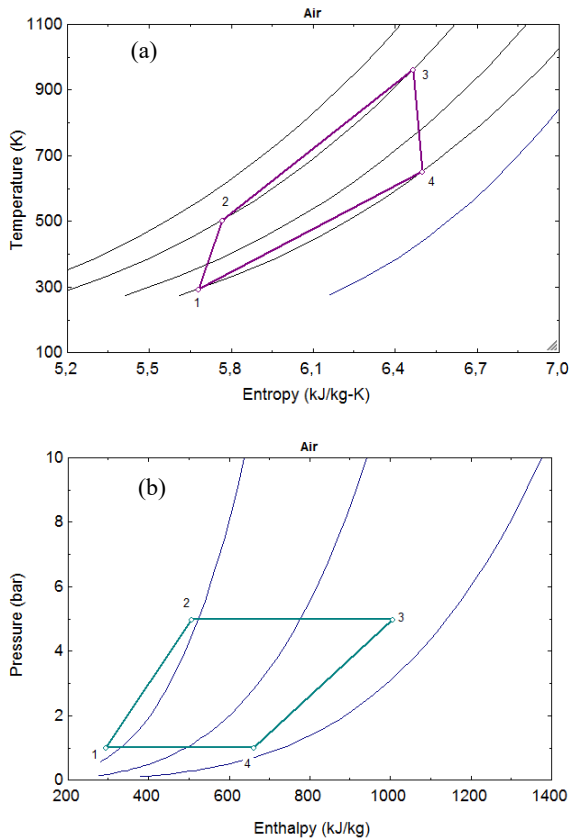


Figure 7: T-s (a) and P-h (b) diagrams of the Brayton cycle of the system 2 (natural gas only).

In order to calculate the exit temperatures of the compressor and the turbine, the isentropic formulas were used:

$$\frac{T_{in,out}}{T_{out,in}} = \left(\frac{P_{in,out}}{P_{out,in}} \right)^{\frac{(k-1)\eta_{is}}{k}} \quad [8]$$

where η_{is} is the isentropic efficiency of the turbine and the compressor and k is the specific heat ratio for air.

The temperature of the product of combustion is calculated as a function of the combustion chamber efficiency η_{thk} , the air-fuel stoichiometric ratio L_{min} , the quantity of excess air l , the mean molar heat capacity C_p , the temperature difference before and after the chamber and the lower heating value of the natural gas LHV (see also Fig. 7):

$$\eta_{thk} = 1 - [(1 + l \cdot L_{min})C_p(T_{15} - T_{14})]/LHV \quad [9]$$

The exhaust gas mass flow \dot{m}_A is estimated by the heat balance equation of the superheater and then it is used to determine the natural gas mass flow \dot{m}_b and the atmospheric air mass flow \dot{m}_a as follows:

$$\dot{m}_A = \dot{m}_b \cdot (1 + l \cdot L_{min}) \text{ and } \dot{m}_a = l \cdot L_{min} \cdot \dot{m}_b \quad [10]$$

Finally, the net power produced by the gas turbine (P_{net}) is determined by the formula below:

$$\dot{m}_a = \frac{P_{net}}{w_{net}} \quad [11]$$

The values of the thermal efficiencies of the cycles and the plant are presented in Table 2.

Table 1: Thermal efficiencies of the systems

| | System 1 | System 2 | System 3 |
|---------------------|----------|----------|----------|
| $\eta_{th,orc}$ | 0,1795 | - | 0.1773 |
| $\eta_{th,brayton}$ | - | 0,226 | 0.2256 |
| $\eta_{th,plant}$ | 0,1735 | 0,226 | 0.2626 |

Finally, the required area of the shell-and-tube heat exchangers are estimated using the LMTD method by an iterative procedure.

4. EXERGY ANALYSIS

In order to carry out the exergy analysis the following state of reference is used: $T(0)=278,15$ K and $P(0)=1$ bar. The enthalpy $h_i(0)$ and the entropy $s_i(0)$ based on the pressure and the temperature are also calculated. Finally, having all the above information the exergy is calculated according to the formula:

$$\dot{E}_i = \dot{m} \cdot (h_i - h_i[0] - T[0] \cdot (s_i - s_i[0])) \quad [12]$$

where \dot{m} is the mass flow of the fluid (either organic or geothermal fluid) and i is the state.

The exergy of the natural gas is:

$$\dot{E}_b = \dot{m}_b \cdot LHV$$

where \dot{m}_b is the mass flow of natural gas.

Regarding the first law efficiency, it is arguably an unrealistic criterion of the components' function. So as to overcome this obstacle, the use of the second law efficiency, known also as exergetic efficiency, is more than necessary. To be more specific, the exergetic efficiency is the ratio of the real thermal efficiency to the maximum thermal efficiency of the component under the same circumstances. A general definition is:

$$\eta_{ex} = \text{useful exergy output / utilized exergy input}$$

However, the exergetic efficiency varies according to the component. For example, the second law efficiency for the turbines is written as:

$$\eta_{ex} = \frac{\dot{W}_t}{(\dot{E}_{in} - \dot{E}_{out})} \quad [13]$$

whereas for the pumps and the compressor is:

$$n_{ex} = \left(\frac{\dot{E}_{out} - \dot{E}_{in}}{\dot{W}} \right) \quad [14]$$

The exergetic efficiencies of the ORC and the plant are defined by the following equation:

$$n_{ex} = \frac{Power_{total} - \dot{W}_{pumps}}{\sum \dot{E}_{fuels,in}} \quad [15]$$

where $\sum \dot{E}_{fuels,in}$ is the sum of the exergy of the fuels at the state of entering the Rankine cycle, the Brayton cycle or the hybrid plants.

It is generally accepted that every process produces entropy and destroys exergy. In other words, the destroyed exergy is proportional to the produced entropy. For the systems of steady flow the following exergy balance equation is used:

$$\sum \left(1 - \frac{T_0}{T_k} \right) \cdot \dot{Q}_k + \dot{W} + \sum \dot{E}_{in} - \sum \dot{E}_{out} - \dot{E}_{d,k} = 0 \quad [16]$$

Thus, the exergy destruction is expressed according to the following formula for every component:

for the turbine

$$\dot{E}_d = 0 + \dot{E}_{in} - \dot{E}_{out} - \dot{W} \quad [17]$$

for the pumps and the compressor

$$\dot{E}_d = 0 + \dot{E}_{in} - \dot{E}_{out} + \dot{W} \quad [18]$$

The total exergy destruction is the sum of exergy destruction of all components.

Another important parameter is the ratio of exergy destruction to the exergy of the fuel that is fed to the system (either geothermal fluid or natural gas).

$$y_{d,k} = \frac{\dot{E}_{d,k}}{\dot{E}_{f,total}} \cdot 100 \quad [19]$$

where

$$\dot{E}_{f,total} = \dot{E}_{geo,in} + \dot{E}_b \quad [20]$$

An alternative formula for the exergy balance for every component is the following:

$$\dot{E}_{F,k} = \dot{E}_{P,k} + \dot{E}_{L,k} + \dot{E}_{d,k} \quad [21]$$

where $\dot{E}_{F,k}$ is the exergy of the fuel fed to every component, $\dot{E}_{P,k}$ is the exergy of the product (the

exergy received from the fluid) and $\dot{E}_{L,k}$ is the exergy loss.

For example, for the compressor the exergy loss is calculated as:

$$\dot{E}_L = \dot{W}_c - (\dot{E}_{out} - \dot{E}_{in}) - \dot{E}_d \quad [22]$$

Finally, the ratio of exergy loss is the exergy loss of every component to the total exergy of the fuels which are fed to the system:

$$y_{L,k} = \frac{\dot{E}_{L,k}}{\dot{E}_{f,total}} \cdot 100 \quad [23]$$

The exergetic efficiencies of the Rankine cycles and the overall plants are presented in Table 2.

Table 2: Exergetic efficiencies (%) of the Rankine cycles and of the plants

| | System 1 | System 2 | System 3 |
|----------------|----------|----------|----------|
| $n_{ex,orc}$ | 40.38 | - | 33.00 |
| $n_{ex,plant}$ | 39.37 | 13.08 | 31.13 |

4. ECONOMIC ANALYSIS

Geothermal plants, as any plant based on renewable energy sources, have a relatively high initial and a low operational cost. The total investment for a geothermal power plant includes the following types of costs: the cost of exploration and verification of resources, the cost of infrastructure, the cost of the power plant which includes the costs of the turbine, heat exchangers as well as pollution abatement systems, and operation and maintenance costs.

The calculation of the total cost of the hybrid system is the most crucial step in the evaluation of the plant's viability. This analysis is based on the labour cost and the cost of raw materials which account for approximately 40% of the final cost, the total capital investment, the cost of fuel (geothermal, natural gas, organic fluid) and the cost of operation and maintenance. In addition to these, the choice of the plant size is a key factor in determining the final cost (e.g. Saibi et al, 2013; Ismail, 2013).

The estimate of the fixed-capital investment (purchased equipment cost, piping cost, land cost etc.) for each system is based on the classical book of Peters et al. (2002).

The hybrid system is going to operate for 335 days or for 8040 hours out of 8760 hours per year. The labour positions will be five with an average hourly wage rate of 15\$/hr for 2080 working hours per year. The cost exploration of the geothermal field and of drilling (two production wells and one reinjection well) (C_{geo}) is estimated at 528000\$ based on the depth of drilling (400 m) for each well. Table 3 presents the capital

investment costs for the three systems considered in this work.

Table 3: Estimate of the total capital investment of the proposed systems in US\$.

| Costs | System 1 | System 2 | System 3 |
|--------------------------------------|-----------|-----------|-----------|
| Total purchased-equipment cost (PEC) | 1,746,000 | 5,496,000 | 3,912,469 |
| Piping (10% of PEC) | 174,647 | 549,618 | 391,247 |
| Total onsite costs | 1,921,000 | 6,046,000 | 4,303,716 |
| Total offsite costs | 11,011 | 11,011 | 11,011 |
| Total direct costs | 1,932,000 | 6,057,000 | 4,314,728 |
| Total indirect costs | 96,606 | 302,840 | 215,736 |
| Fixed capital investment (FCI) | 2,029,000 | 6,360,000 | 4,530,464 |
| Total other outlays | 534,249 | 1,107,000 | 804,683 |
| Total capital investment | 2,563,000 | 7,466,000 | 5,335,147 |

5.1 Exergy costing

The capital investment rate, $Z_{CI,k}$, of the k-th component of the plant is calculated (in \$/s) as:

$$\dot{Z}_{CI,k} = \frac{CRF}{t_{op}} \cdot C_{eq,k} \cdot (1 + r_n)^2 \quad [24]$$

The operation and maintenance cost rate, $Z_{O\&M,k}$, of the k-th component of the plant is calculated as:

$$\dot{Z}_{O\&M,k} = \frac{CRF \cdot C_{L,OM} \cdot C_{eq,k}}{t_{op} \cdot C_{PEC}} \quad [25]$$

where $C_{L,OM}$ is the annual levelised operation and maintenance cost.

The total cost rate of a component therefore is:

$$\dot{Z}_k = \dot{Z}_{CI,k} + \dot{Z}_{O\&M,k}$$

The cost balance in the components of the plant can be expressed as:

$$\dot{C}_{P,k} = \dot{C}_{F,k} + \dot{Z}_{CI,k} + \dot{Z}_{O\&M,k} \quad [26]$$

where $\dot{C}_{P,k}$ is the component's product cost flow (\$/s) and $\dot{C}_{F,k}$ is the component's fuel cost flow (\$/s).

The cost flows $\dot{C}_{P,k}$ and $\dot{C}_{F,k}$ are expressed as a function of the levelised cost rates \dot{C}_i (\$/s) which in turn are a function of exergy rates of fluid states \dot{E}_i (kW) multiplied by their corresponding coefficients c_i

(\$/kJ), which are called levelised unit costs of exergy. A typical set of the results is presented in Table 4 for the System 1.

Table 4: Pressure, temperature, enthalpy, entropy, exergy rate, levelised cost of exergy unit and levelised cost rate for each state of the fluids in System 1.

| State | P_i (bar) | T_i (K) | h_i (kJ/kg) | s_i (kJ/kgK) | E_i (kW) | c_i (\$/kJ) | C_i (\$/s) |
|-------|----------------|-----------|------------------|-------------------|---------------|------------------|-----------------|
| 0 | 1 | 293 | | | | | |
| 1 | 2.5 | 363 | 376.4 | 1.191 | 1.691 | 2.34E-07 | 0.000396 |
| 2 | 25 | 363 | 378.2 | 1.189 | 1.814 | 2.34E-07 | 0.000425 |
| 3 | 13 | 261 | 173.4 | 0.8933 | 1.495 | 0.0140 | 21 |
| 4 | 22 | 299 | 111.9 | 0.3834 | 132.6 | 2.34E-07 | 0.000031 |
| 5 | 12.5 | 355 | 666.6 | 2.397 | 3.075 | 0.0140 | 43.21 |
| 6 | 12.2 | 455 | 902.5 | 2.984 | 4.988 | 0.0140 | 70.08 |
| 7 | 1.017 | 388 | 769.2 | 3.01 | 764 | 0.0140 | 10.73 |
| 8 | 1 | 261 | 172.4 | 0.8971 | 1.431 | 0.0140 | 20.1 |
| 9 | 1 | 278 | 20.49 | 0.07399 | 1.423 | 0.0117 | 16.69 |
| 10 | 1 | 283 | 41.46 | 0.1487 | 624.1 | 0.0117 | 7.321 |
| 11 | 1 | 293 | 293.4 | 5.682 | 4.803 | 0 | 0 |
| 12 | 1 | 754 | 771.3 | 6.656 | 7.908 | 1.469E-05 | 0.1161 |
| 13 | 1 | 293 | 293.4 | 5.682 | 5.057 | 1.469E-05 | 0.0743 |
| b | | | | | 34.26 | 0.339E-05 | |

The fuel and product unit costs ($c_{F,k}$ and $c_{P,k}$ in \$/kg) of the k-th component are determined by the cost balance.

The exergy destruction cost rates $\dot{C}_{D,k}$ (\$/s) in each component are calculated by the following equation:

$$\dot{C}_{D,k} = c_{F,k} \cdot \dot{E}_{D,k} \quad [27]$$

Furthermore, the relative cost difference r_k represents the relative increase in the average cost per exergy unit between the fuel and the product of each component. It is determined by the equation:

$$r_k = \frac{c_{F,k} \cdot (\dot{E}_{D,k} + \dot{E}_{L,k}) + \dot{Z}_k}{c_{F,k} \cdot \dot{E}_{P,k}} \quad [28]$$

Another important variable is the exergoeconomic factor f_k of each component that compares the investment, operation and maintenance cost (non-exergy related) to the total cost (exergy and non-exergy related). This factor is an estimate of the greatest source of expenditure of the plant.

$$f_k = \frac{\dot{Z}_k}{\dot{Z}_k + c_{F,k} \cdot (\dot{E}_{D,k} + \dot{E}_{L,k})} \quad [29]$$

The yearly income of the plant (before taxation), C_{income} , is calculated as a function of the total revenue

from the electricity, the operation and maintenance cost of the geothermal field and the annual levelised operation and maintenance cost of the plant (\$/year):

$$C_{income} = C_{electricity} - C_{L,O\&M,geo} - C_{L,O\&M} \quad [30]$$

where $C_{electricity} = \sum c_{w,t} \cdot t_{op} \cdot \dot{W}_t$.

The unit cost of the power produced ($ucpp$) is defined by the following equation in cents/kWh:

$$ucpp = \left(\dot{Z}_{Cl,total} + \dot{Z}_{O\&M,total} + \dot{C}_{f,total} \right) \cdot t_{op} \cdot 100 / \left(P_{net} + \dot{W}_t \right) \cdot 8040 \quad [31]$$

where $\dot{C}_{f,total}$ is the total sum of the cost rates \dot{C}_i of the system's fuels (the geothermal fluid and/or the natural gas) at their entry state to the system.

6. EVALUATION OF THE SYSTEMS

The thermoeconomic evaluation of the proposed plants is based on the values of the exergetic efficiency $n_{ex,k}$, the exergy destruction and loss ratios $y_{D,k}$ and $y_{L,k}$, the relative cost difference r_k , the exergoeconomic factor f_k and the value of $\dot{Z}_k + \dot{C}_{D,k}$ for each component. This evaluation was carried out using the EES software and the results for the three systems are presented in Figures 5-7.

Table 5: Values of various evaluation parameters for the System 1.

| Component | $n_{ex,k}$ | $y_{D,k}$ (%) | $y_{L,k}$ (%) | r_k | f_k (%) | $\dot{Z}_k + \dot{C}_{D,k}$ (\$/s) |
|-------------|------------|---------------|---------------|--------|-----------|------------------------------------|
| Turbine 1 | 0.9471 | 0.622 | 0 | 0.0560 | 0.2344 | 3.15 |
| Feed pump | 0.8676 | 0.0272 | 0 | 0.1527 | 0.0962 | 0.119 |
| Hpp | 0.8372 | 0.0666 | 0 | 1.608 | 87.91 | 0.000212 |
| Evaporator | 0.9401 | 0.278 | 0 | 0.8701 | 92.68 | 0.00032 |
| Superheater | 0.6703 | 2.616 | 0 | 0.5028 | 2.178 | 0.0141 |
| Condenser | 0.8348 | 0.367 | 3.71 | 2.198 | 0.00274 | 1.55 |
| C. chamber | 0.2024 | 86.65 | 0 | 3.941 | 0.0478 | 0.106 |
| Total | 0.3937 | 90.63 | 3.71 | - | - | 4.94 |

Table 6: Values of various evaluation parameters for the System 2.

| Component | $n_{ex,k}$ | $y_{D,k}$ (%) | $y_{L,k}$ (%) | r_k | f_k (%) | $\dot{Z}_k + \dot{C}_{D,k}$ (\$/s) |
|------------|------------|---------------|---------------|--------|-----------|------------------------------------|
| Turbine 2 | 0.9252 | 1.137 | 0 | 0.2096 | 61.44 | 0.02451 |
| Compressor | 0.8881 | 0.9797 | 0 | 1.252 | 89.93 | 0.01201 |
| C. chamber | 0.2919 | 85.75 | 0 | 2.427 | 0.01872 | 0.2518 |
| Total | 0.1306 | 87.87 | 0 | - | - | 0.28832 |

Exergetic efficiencies

In the hybrid system (ORC without Brayton) the exergetic efficiency of the plant is 39.4%, which is

quite high in comparison with the thermal efficiency of the plant which is 17.4 %.

In the Brayton system the plant's exergetic efficiency is the lowest among the three systems.

In the hybrid system (ORC and Brayton) the exergetic efficiency of the plant it is 31.1%, which can be considered as acceptable compared with the thermal efficiency which is 26.26%.

Table 7: Values of various evaluation parameters for the System 3.

| Component | $n_{ex,k}$ | $y_{D,k}$ (%) | $y_{L,k}$ (%) | r_k | f_k (%) | $\dot{Z}_k + \dot{C}_{D,k}$ (\$/s) |
|-------------|------------|---------------|---------------|--------|-----------|------------------------------------|
| Turbine 1 | 0.9382 | 0.5548 | 0 | 0.0661 | 0.2134 | 2.445 |
| Turbine 2 | 0.924 | 1.096 | 0 | 0.2635 | 68.76 | 0.01046 |
| Compressor | 0.8821 | 0.9762 | 0 | 1.267 | 89.45 | 0.005766 |
| Feed pump | 0.8676 | 0.0209 | 0 | 0.1527 | 0.1029 | 0.07959 |
| Hpp | 0.8372 | 0.0765 | 0 | 10.72 | 98.19 | 0.000179 |
| Evaporator | 0.7459 | 1.147 | 0 | 0.5359 | 36.43 | 0.000716 |
| Superheater | 0.7719 | 1.204 | 0 | 0.3145 | 6.023 | 0.00382 |
| Condenser | 0.8176 | 0.311 | 2.789 | 2.223 | 0.0029 | 1.119 |
| C. chamber | 0.2922 | 81.51 | 0 | 2.424 | 0.0553 | 0.08644 |
| Total | 0.3113 | 86.9 | 2.789 | | | 3.75 |

Exergy destruction and loss ratios

The exergy destruction and loss ratios indicate the percentage of exergy destructed or wasted in each component and whether it should be replaced or not.

Relative cost difference

It can be seen that the relative cost difference is low for most of the components of the three systems, which makes the choice of the majority of the components suitable.

Exergoeconomic factors

When an exergoeconomic factor is very low, it is an indicator that the exergy-related costs are much higher in comparison with the investment and operation costs and, as a result, the component should be replaced with another that has better exergetic efficiency. On the other hand, when it is very high, it may suggest that the non-exergy related costs are much higher than the exergy-related ones and the component should be replaced with a cheaper one.

Cost rates of the components

In order to improve the cost effectiveness of the hybrid system the evaluation of the following indicator $\dot{Z}_k + \dot{C}_{D,k}$ is necessary. The components with the highest value are the least economically profitable choices thus the plant's economic viability is determined by the sum of $\dot{Z}_k + \dot{C}_{D,k}$, a term that composes the total cost rate for every component.

Overall evaluation

The final comparison of the three systems, based on the abovementioned results, is presented in Table 8.

Table 8: Comparison of the three systems.

| | System 1 | System 2 | System 3 |
|---|-----------|-----------|-----------|
| <i>Produced electricity from geothermal resources</i> | 4,000 | 0 | 2,634 |
| <i>Produced electricity from natural gas</i> | 0 | 4,000 | 1,366 |
| <i>Total capital investment</i> | 2,563,000 | 7,466,000 | 5,335,147 |
| <i>C_{income} (\$/year)</i> | 1,717,611 | 1,133,698 | 1,142,233 |
| <i>ucpp (US cents/kWh)</i> | 11.27 | 9.427 | 10.9 |

The binary system with natural gas superheating has 4 MWe output based mainly on geothermal resources. Enviously, the system of the natural gas plant has 4 MW output without taking advantage of any renewable resources. Finally, the system that combines both Brayton and Rankine cycles, System 3, produces 2.634 MW of electricity due to geothermal utilisation and 1.366 MW of electricity from natural gas.

Regarding the comparison of the systems in terms of cost, the first one is the most profitable of all as the total capital investment is 2,563,000 \$ and the yearly income before taxation is 1,717,611 \$. In the second system, however there is the greatest total capital investment 7,466,000 \$ and the lowest yearly income, 1,333,698 \$. In the hybrid ORC and Brayton system the total capital investment is noticeably higher than the first hybrid system 5,335,147\$ and the yearly income is less than the first system, to be specific 1,142,233 \$. Hence, the two geothermal systems are much more favorable.

At this point, the importance of the unit cost of power produced should be underlined, because it is a crucial factor to the viability of every plant. The first system, even though it has the highest *ucpp* (11.27 cents/kWh) amongst the three systems, it has the best and most appealing financial aspects and all the produced electricity comes from geothermal resources with a small contribution of natural gas. On the other hand, the *ucpp* in the hybrid ORC and Brayton system is lower than the previous system (10.9 cents/kWh). However, the natural gas plays a major role in the production of electricity and, consequently, it can be considered as a much less environmentally-friendly energy system. Finally, the second system has the lowest *ucpp* (9.427 cents/kWh), which is anticipated as natural gas is widely used for power production due to the fact that it is less expensive and more environmentally-friendly than coal, yet it is not a sustainable energy resource.

6. CONCLUSIONS

The scope of this paper was to evaluate the viability of hybrid systems that combine low-temperature geothermal energy sources with natural gas. The results of the energetic and economic analysis of the systems considered here suggest that this combination is appealing and steps should be taken in order to introduce geothermal energy more actively in the electricity production sector in Greece, where currently there is no electricity production based on geothermal energy.

In particular, for the first system the exergetic efficiency is 39.4%, which proves that this system is competitive since it exploits much more of the exergy input in comparison with the third system. However, this efficiency may seem low compared with other geothermal plants. On the other hand, this efficiency looks like to be more than satisfactory considering the low input temperature of the resource (90°C). So as to enhance even more the overall exergetic efficiency some components that were proven ineffective by the exergetic evaluation should be replaced.

In terms of thermoeconomic analysis the hybrid geothermal system with natural gas superheating requires the lowest capital investment and yields the greatest yearly income.

Although the plant is based on geothermal energy, it is not 100% environmentally-friendly, since the contribution of natural gas to electricity production is undeniably important. Therefore, in order to render the hybrid system less dependent on fossil fuel, it is proposed to replace natural gas with biogas. Furthermore, so as to produce more power, there are many options to strengthen the system, some of which are solar energy, biomass etc.

REFERENCES

- Andritsos, N., Dalambakis P., Arvanitis, A., Papachristou, M. and Fytikas M.: Geothermal Development in Greece-Country update 2010-2014, *Proceedings of the World Geothermal Congress 2015*, Melbourne, Australia, (2015), paper #01048, 1-11.
- DiPippo R. Geothermal power plants: evolution and performance assessments. *Geothermics* 2015; 53: 291–307.
- DiPippo, R.: *Geothermal Power Plants, Principles, Applications, Case Studies and Environmental Impact*, Butterworth-Heinemann, Third Edition, (2012).
- Fytikas, M., and Kolios, N.: Geothermal exploration in the west of the Nestos delta, *Acta Vulcanologica*, Marinelli Volume, 2, 237-246 (1992)
- Ismail, B.I.: Chapter 13: ORC-Based Geothermal Power Generation and CO₂-Based EGS for Combined Green Power Generation and CO₂ Sequestration in New developments in renewable

- energy, in *New Developments in Renewable Energy*, H. Arman and I. Yuksel (eds.), Intech, (2013).
- Kolios, N., Fytikas, M., Arvanitis, A., Andritsos, N. and Koutsinos, S.: Prospective medium-enthalpy geothermal resources in sedimentary basins of Northern Greece, *Proceedings of the European Geothermal Congress 2007*, Unterhaching, Germany, (2007), paper #258, 1-11.
- Kolios, N., Koutsinos, S., Arvanitis, A., Karydakis, G.: Geothermal Situation in North-eastern Greece, *Proceedings World Geothermal Congress 2005*, Antalya, Turkey, (2005), paper #2614, 1-14.
- Mendrinou, D., Choropanitis, I., Polyzou, O., Karytsas, C.: Exploring for geothermal resources in Greece, *Geothermics*, 39, (2010), 124-137.
- Peters, M., Timmerhaus, K., West, R.: *Plant Design and Economics for Chemical Engineers*, McGraw-Hill, 5th Edition, (2002).
- Romagnoli, P.: The Italian experience in the geothermal fields exploitation. Presented at the Iceland Geothermal Congress 2016, Reykjavik, 26-29 April, 2016.
- Saibi, H., Finsterle, S., Bertani, R., Nishijima, J.: Geothermal Energy, in *Handbook of Sustainable Engineering*, J. Kauffman, K.-M. Lee (eds.), *Springer Science+Business Media*, Dordrecht (2013).

Acknowledgements

The paper is dedicated to the memory of our friend, colleague and teacher Prof. Anastasios Stamatis, who passed away on May 20, 2015. He has contributed in this work with many ideas and suggestions.